Morphological Classification of the Medial Frontal Cortex Based on Cadaver Dissections: A Guide for Interhemispheric Approach

Yasutaka IMADA,[1] Toru TAKUMI,[2,3] Hirohiko AOYAMA,[4,5]
Takashi SADATOMO,[6] and Kaoru KURISU[7,8]

[1]Department of Neurosurgery, Yamada Memorial Hospital, Mihara, Hiroshima, Japan
[2]Department of Integrative Bioscience, Graduate School of Biomedical and Health Sciences, Hiroshima University, Hiroshima, Hiroshima, Japan
[3]Department of Physiology and Cell Biology, Kobe University School of Medicine, Kobe, Hyogo, Japan
[4]Department of Anatomy and Developmental Biology, Graduate School of Biomedical and Health Sciences, Hiroshima University, Hiroshima, Hiroshima, Japan
[5]Faculty of Health Science, Hiroshima International University, Higashihiroshima, Hiroshima, Japan
[6]Department of Neurosurgery, Higashihiroshima Medical Center Higashihiroshima, Hiroshima, Japan
[7]Department of Neurosurgery, Graduate School of Biomedical and Health Sciences, Hiroshima University, Hiroshima, Hiroshima, Japan
[8]Department of Neurosurgery, Chugoku-Rosai Hospital, Kure, Hiroshima, Japan

Abstract

The medial frontal cortex (MFC) is a part of the medial surface of the frontal lobe situated in the rostral portion of the corpus callosum (CC). In a surgical interhemispheric approach (IHA), the MFC covers the anterior communicating artery (Aco) complex until the final stage of dissection. To clarify the anatomical relationship between the MFC and the Aco complex, and to facilitate orientation in IHA, we analyzed the morphological features of the MFC in number, size, and pattern of gyri from the medial surface of the hemisphere in the subcallosal portion using 53 adult cadaveric hemispheres. The mean width of the MFC excluding cingulate gyrus (MFCexcg) was 20.6 ± as mm in the subcallosal portion. MFCexcg consisting of 2, 3, 4, or 5 gyri were observed in 7.5%, 56.6%, 32.1%, or 3.8% of the hemispheres, respectively. Bilateral MFCexcg consisting of >2 gyri were observed in approximately 85% of the hemispheres. Therefore, in many cases, the dissection performed at 2 cm upward from the base of the straight gyrus (SG) or 3–4 gyri of the MFC is sufficient to safely reach the upper portion of the cistern of lamina terminalis located distal to the Aco complex in IHA. The MFC is a good landmark for intraoperative orientation in IHA.

Keywords: medial frontal cortex, cingulate gyrus, interhemispheric fissure, interhemispheric approach, basal interhemispheric approach

Introduction

In the interhemispheric approach (IHA), the interhemispheric fissure (IHF) should be dissected carefully along with the ventral part of the bilateral medial frontal cortex (MFC) to prevent postoperative neuropsychological impairment by severe damage of it. The MFC represents the medial wall of the frontal lobe situated near the rostral portion of the corpus callosum (CC), and is implicated in not only memory learning but also social, cognitive, and affective functions.[1] The sulcal patterns of the ventral part of the MFC are diverse.[2–13] The strength of adhesion of the bilateral hemispheres at the IHF

is often the focus of attention during dissection in IHA, while the morphological features of the MFC may be ignored. Usually, the genu of the CC, the pericallosal artery, and the tuberculum sellae are used as landmarks in IHA to reach the cistern of lamina terminalis and the anterior communicating artery (Aco) complex. However, it is difficult to estimate accurately the position of the Aco complex during dissection, because the Aco complex is covered by MFC until the final stage of dissection in the IHA operative field. Therefore, especially in a basal interhemispheric approach (BIHA), it is difficult to judge the efficient dissecting range of the MFC to reach the upper portion of the cistern of lamina terminalis located distal to the Aco complex. However, few reports have discussed these anatomical relationships.[14,15] In this study, we analyzed the morphological features of the MFC in number, size, and pattern of gyri using cadaveric dissections and investigated the anatomical relationship between the MFC and the upper portion of the cistern of lamina terminalis located distal to the Aco complex. Our results indicate that the gyri of MFC are good landmarks to safely reach the upper portion of the cistern of lamina terminalis located distal to the Aco complex and to obtain intraoperative good orientation during IHA.
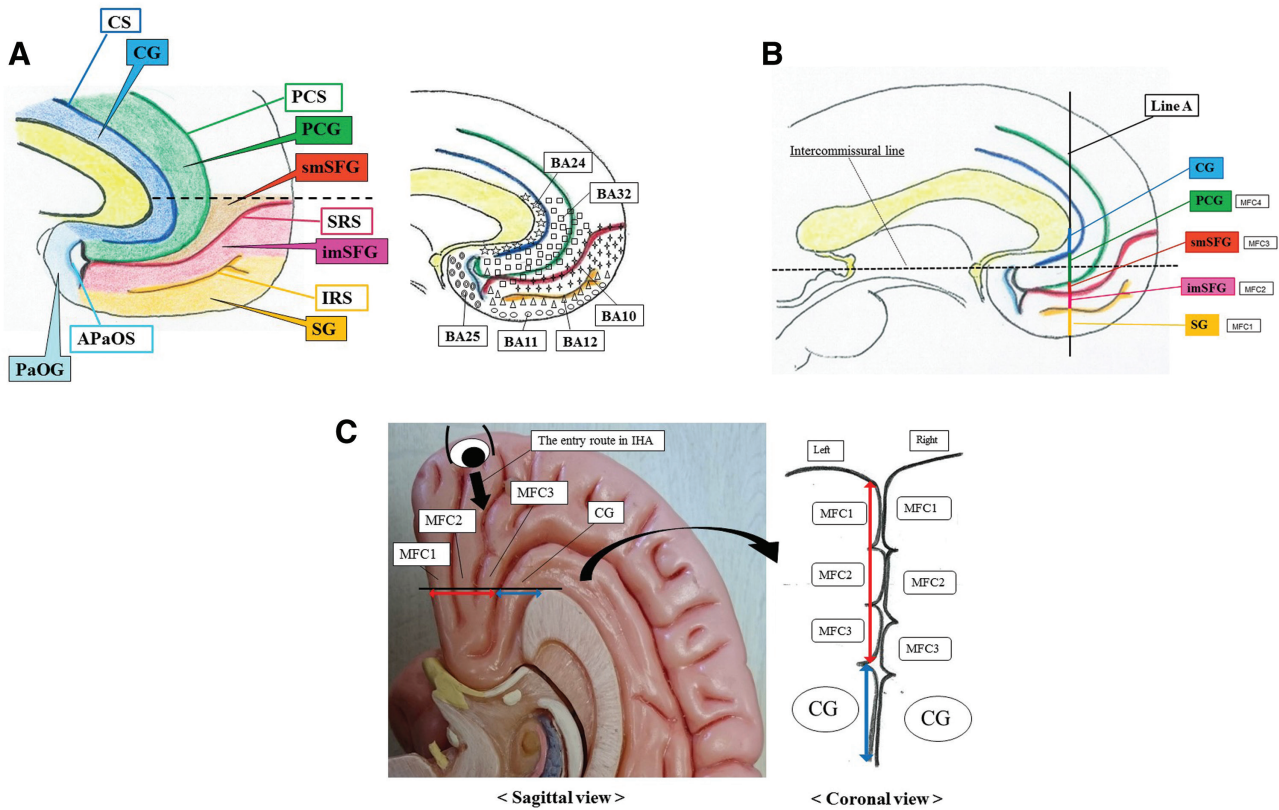
Nomenclature

The MFC represents the medial wall of the frontal lobe which mainly contains the medial aspects of the superior frontal gyrus (SFG), the cingulate gyrus (CG), the straight gyrus (SG) and the paraolfactory gyrus (PaOG). In this study, we define the ventral part of the MFC (ventral MFC) as the area ventral to the imaginary line drawn horizontally from the genu toward the frontal pole (Fig. 1a). The ventral MFC mainly consists of the Brodmann area (BA) 10, 11, 12, 24, 25, 32, and 33[16–18] (Fig. 1a), and the sulcal patterns are diverse.[2–13] We basically adopt the anatomical terms based on the *Terminologia Neuroanatomica* (TNA, 2017: http://FIPAT.library.dal.ca). TNA is a revision of the terminology on the central nervous system in the *Teminologia Anatomica* (TA, 1998) that was made by the Working Group Neuroanatomy of the Federative International Programme for Anatomical Terminology (FIPAT) of the International Federation of Associations of Anatomists (IFAA).[19] However, some sulci and gyri of the ventral MFC are not listed in the TNA, and their anatomical terms are controversial among the researchers.[2–13,19] Especially, the definition of the superior rostral sulcus (SRS) and the inferior rostral sulcus (IRS) on the ventral MFC is clearly different between Ono et al[5] and Economo et al.[18] The former

has been adopted mainly by anatomists[2–4,6–8,19] and the latter by researchers of the cortical architecture or the functional neuroimaging.[9,11–13] In this study, we also follow the nomenclature of Ono et al.[5] The SRS is the first major horizontal sulcus ventral to the CC. The IRS is the sulcus ventral to the SRS and separates the SG from the medial aspect of the SFG. An additional sulcus, ventral to the IRS, was observed in several subjects, but was not labeled by Ono.[5] The paracingulate sulcus (PCS), which extends dorsally and parallel to the CS, is often present. The paracingulate gyrus (PCG) is the gyrus between the CS and the PCS. Although a few terms can be seen among the researchers,[11,12] there are no established anatomical terms to represent the gyri between the CS or the PCS and the IRS. The area consists of the medial aspect of the SFG which mainly contains the BA 10.[16–18] Therefore, we tentatively label the gyrus between the CG or the PCS and the SRS as the superior medial segment of the SFG (smSFG), and the gyrus between the SRS and the IRS as the inferior medial segment of the SFG (imSFG). In the case that the sulcus ventral to the IRS is present, we tentatively label the gyrus below it as the SG1, and the gyrus above it as the SG2 (Fig. 1a).

Materials and Methods

The sulcal patterns of ventral MFC were observed in 27 adult cadaveric brains (total 53 hemispheres; Right: 26, Left: 27) that were prepared for medical student dissection in 2012. One of the right hemispheres could not be used due to severe damage.

First, we identified the sulci and the gyri on the ventral MFC. The identified sulci were the CS, PCS, SRS, IRS, and sulcus ventral to the IRS. The identified gyri in the subcallosal portion were the CG, PCG, smSFG, imSFG, and SG (SG1, SG2). Second, the width of each gyrus was measured from the anterior margin of the callosal genu along a line drawn perpendicularly to the intercommissural line on the medial surface of the hemispheres (Figs. 1a and 1b). In addition, we identified that the MFC excluding CG (MFCexcg) was formed from 2 to 5 small gyri at the subcallosal portion. For convenience, we identified them as MFC1, MFC2, MFC3, MFC4, and MFC5, respectively, in order from the outermost layer in sagittal view, instead of the anatomical name (Fig. 1b). Figure 1c is a medial view of the MFC in the sagittal plane and an upside down coronal view in which the superior side is the cranial bottom. The eye-mark shows the actual intraoperative direction in IHA (Fig. 1c). Width

Fig. 1 (A) Nomenclature of the medial surface of the anterior hemisphere and the relationship between the MFC and BA. Ventral MFC is an area below the black wavy line which is an imaginary line drawn horizontally from the genu toward the frontal pole. (B) Measurement of the width of each gyrus of the MFC. The width of each gyrus of the MFC was measured at Line A. Line A is a line drawn perpendicularly to the intercommissural line from the anterior margin of the callosal genu on the medial surface of the hemispheres. MFC excluding CG (MFCexcg) consists of 2–5 small gyri at the subcallosal portion and each gyrus is defined as MFC1, MFC2, MFC3, MFC4, and MFC5 in order from the outermost layer. (C) Anatomical view of the MFC. This image shows the medial view of the MFC in the sagittal plane and an upside down coronal view in which the superior side is the cranial bottom. This coronal view corresponds to the actual operative findings in IHA. The eye-mark shows the actual intraoperative direction in IHA. APaOS: anterior paraolfactory sulcus, CG: cingulate gyrus, CS: cingulate sulcus, IHA: interhemispheric approach, imSFG: inferior medial segment of SFG, IRS: inferior rostral sulcus, MFC: medial frontal cortex, PaOG: paraolfactory gyrus, PCG: paracingulate gyrus, PCS: paracingulate sulcus, SG: straight gyrus, smSFG: superior medial segment of SFG, SRS: superior rostral sulcus.

data of each gyrus of the MFC were demonstrated as the mean ± standard deviations (SD) (Table 1). Finally, we observed the numbers of the bilateral gyri of the MFC in the subcallosal portion and demonstrated their patterns in the upside down coronal view. As a result of discussions with Institutional Review Board of Graduate School of Biomedical and Health Sciences, Hiroshima University and Department of Neurosurgery, Graduate School of Biomedical and Health Sciences, Hiroshima University, in this report, we demonstrate the anatomical figures of the MFC without any photographs of cadaveric cerebral hemispheres because of an ethical considerations.

Results

Details of the sulcal patterns of the ventral MFC are shown in Fig. 2a. The PCS was present in 81% of the hemispheres (Type B1, C1, C2, D), with 73% and 89% in the right and left hemispheres, respectively. The SRS and the IRS were present in all hemispheres. The sulcus ventral to IRS was present in 34% (Type B2, C2, C3, D), with 23% and 44% in the right and left hemispheres, respectively. The anterior origin of the CS or the PCS with a connection to the SRS, that is, the pattern which the smSFG was not found in the subcallosal portion, was present in 83%

Table 1 Summary of the variations and width of the MFC

	Total hemispheres	Hemispheres with MFCexcg consisting of 2 gyri	Hemispheres with MFCexcg consisting of 3 gyri	Hemispheres with MFCexcg consisting of 4 gyri	Hemispheres with MFCexcg consisting of 5 gyri
	N = 53	N = 4 (7.5%) Right: n = 2 Left: n = 2	N = 30 (56.6%) Right: n = 17 Left: n = 13	N = 17 (32.1%) Right: n = 7 Left: n = 10	N = 2 (3.8%) Right: n = 0 Left: n = 2
MFC1 (mean±SD)		8.3 ± 2.1 mm	6.3 ± 1.7 mm	6.4 ± 1.5 mm	5.5 ± 0.7 mm
MFC2 (mean±SD)		6.8 ± 3.0 mm	5.7 ± 1.6 mm	5.1 ± 1.5 mm	5.5 ± 0.7 mm
MFC3 (mean±SD)		-	7.5 ± 1.5 mm	4.7 ± 1.7 mm	3.5 ± 2.1 mm
MFC4 (mean±SD)		-	-	7.4 ± 1.7 mm	3.5 ± 2.1 mm
MFC5 (mean±SD)		-	-	-	5.0 ± 2.8 mm
MFCexcg (mean±SD)	**20.6 ± 3.4 mm**	**15.0 ± 1.2 mm**	**19.6 ± 2.5 mm**	**23.5 ± 2.6 mm**	**23.0 ± 1.4 mm**
CG (mean±SD)	7.2 ± 3.2 mm	13.0 ± 2.5 mm	8.1 ± 2.2 mm	4.6 ± 2.3 mm	5.0 ± 2.8 mm

CG: cingulate gyrus, MFC: medial frontal cortex, MFCexcg: MFC excluding CG, SD: standard deviation.

(Type A,B1,B2,C2), with 77% and 89% in the right and left hemispheres, respectively.

The mean width of the MFCexcg was 20.6 ± 3.4 mm and that of the CG was 7.2 ± 3.2 mm in the subcallosal portion (Table 1). The variations of the MFC are shown in Table 1. MFCexcg consisting of 2 gyri were observed in 7.5% (N = 4; Right: n = 2, Left: n = 2) of the hemispheres. The mean width of the MFCexcg was 15±1.2 mm, including the MFC1 (8.3 ± 2.1 mm), and the MFC2 (6.8 ± (6 mm). The mean width of the CG was 13 ± 2.5 mm. MFCexcg consisting of 3 gyri were observed in 56.6% (N = 30; Right: n = 17, Left: n = 13) of the hemispheres. The mean width of the MFCexcg was 19.6 ± 2.5 mm, including the MFC1 (6.3 ± (6 mm), the MFC2 (5.7 ± (5 mm), and the MFC3 (7.5± (7 mm). The mean width of the CG was 8.1 ± .1 mm. MFCexcg consisting of 4 gyri were observed in 32.1% (N = 17; Right: n = 7, Left: n = 10) of the hemispheres. The mean width of the MFCexcg was 23.5 ± was mm, including the MFC1 (6.4 ± 1.5 mm), the MFC2 (5.1 ± 1.5 mm), the MFC3 (4.7 ± 1.7 mm), and the MFC4 (7.4 ± (7 mm). The mean width of the CG was 4.6 ± 2.3 mm. MFCexcg consisting of 5 gyri were observed in 3.8% (N = 2; Right: n = 0, Left: n = 2) of the hemispheres. The mean width of the MFCexcg was 23 ± 1.4 mm, including the MFC1 (5.5 ± (5 mm), the MFC2 (5.5 ± (5 mm), the MFC3 (3.5 ± (3 mm), the MFC4 (3.5 ± (3 mm), and the MFC5 (5.0 ± 2.8 mm). The mean width of the CG was 5.0 ± .0 mm.

Figure 2b shows the patterns of the bilateral MFCexcg. Patterns consisting of 2 gyri and 3 gyri of opposing MFCexcg were observed in two cases (7.7%). Patterns consisting of 2 gyri and 4 gyri of opposing MFCexcg were observed in two cases (7.7%). Patterns consisting of 3 gyri and 3 gyri of opposing MFCexcg were observed in eight cases (30.8%). Patterns consisting of 3 gyri and 4 gyri of opposing MFCexcg were observed in nine cases (34.6%). Patterns consisting of 3 gyri and 5 gyri of opposing MFCexcg were observed in two cases (7.7%). Patterns consisting of 4 gyri and 4 gyri of opposing MFCexcg were observed in three cases (11.5%). Thus, in approximately 85% cases, both MFCexcg consisted of 3 gyri and more. Over all, there was no statistical significance between right and left numbers of the gyri of MFCexcg (Table 1, Typing $\chi 2$ = 3.045, p >0.3847).

Discussion

The ventral MFC has been involved in a variety of social, cognitive, and affective functions. There has been a huge research studies on them.[1,20,21] BA24/25/32 in the region of the ventral MFC is involved in emotion, motivation, and interpersonal behavior,[20,22] especially BA32 is involved in affective valence.[23] Placebo effects and expectations for reduced pain increase the activity of BA24/32 in the region of the ventral MFC.[24–26] BA10 and a part of BA32 in
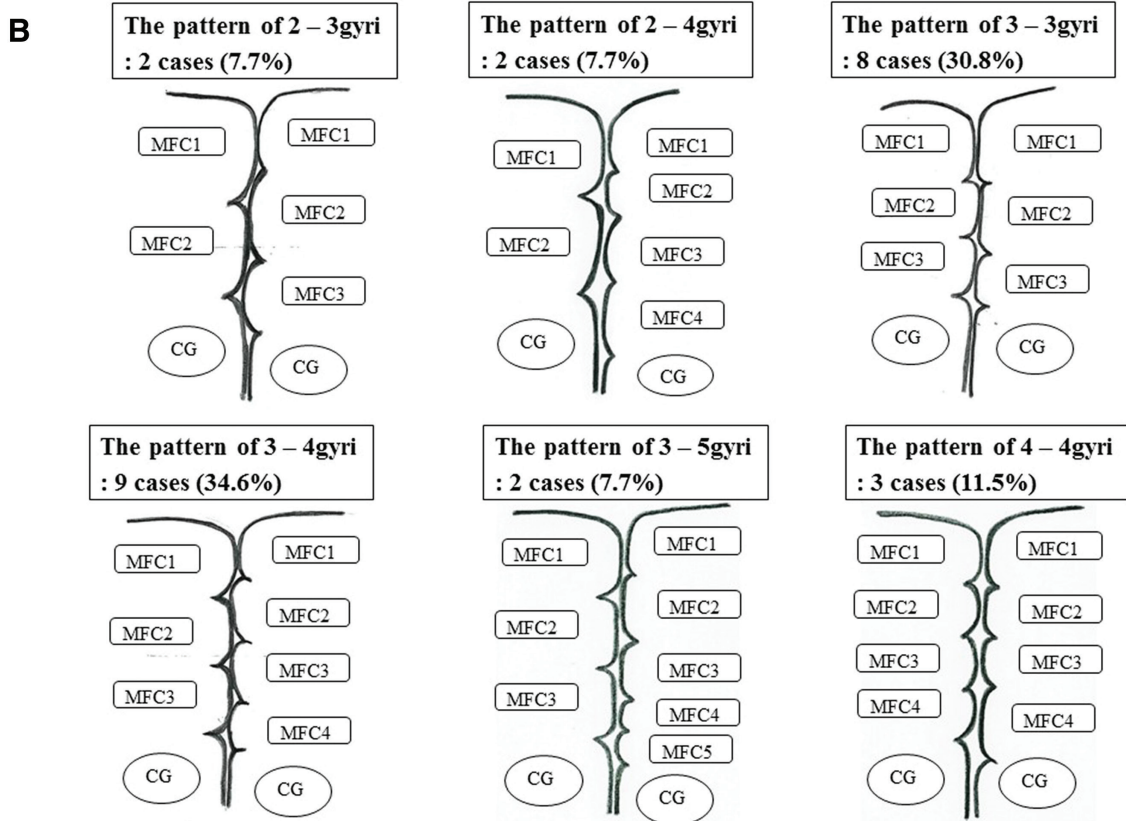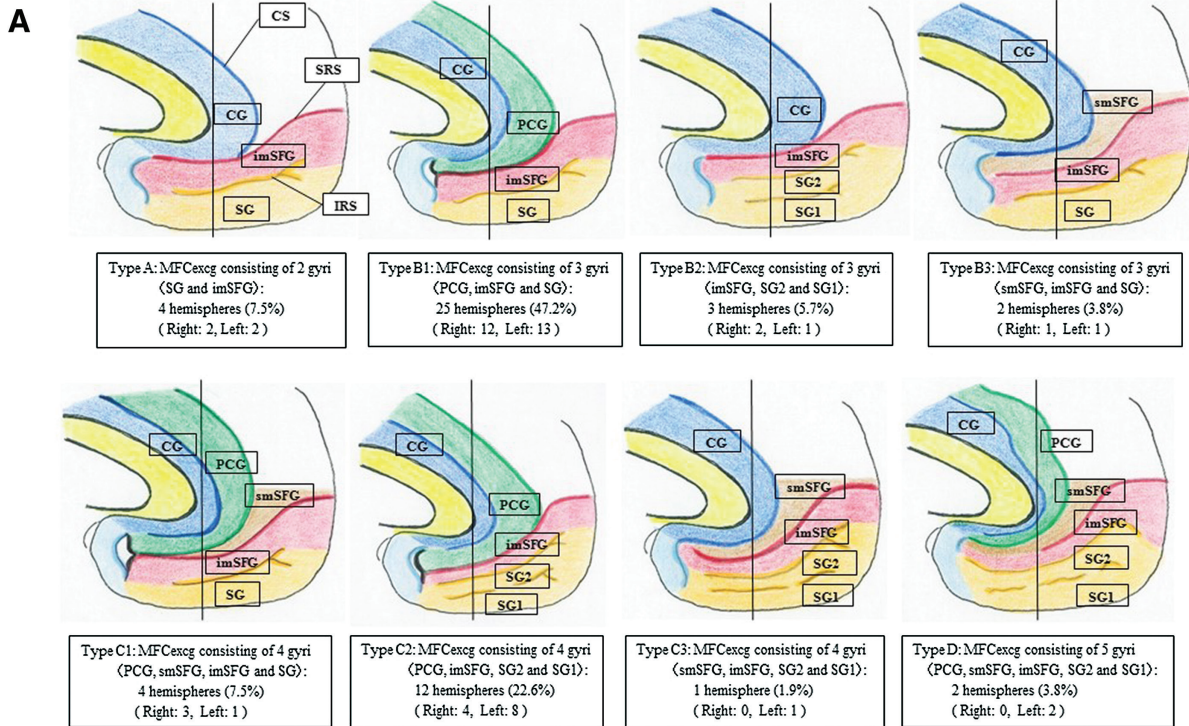
Fig. 2 (A) Schema shows the results of the pattern of the MFC in the sagittal view. (B) The patterns of numbers of the bilateral components of MFCexcg in the subcallosal portion are demonstrated in an upside down coronal view. MFCexcg, Medial frontal cortex excluding cingulate gyrus.

the region of the ventral MFC is involved in the subgoal processing to achieve higher-order action goals,[27–29] and intentional recall of episodic memory.[30–32] BA10/12/32 in the region of the ventral MFC is involved in value and decision-making, especially response to positive rewards.[33–41] BA10/12 in the region of the ventral MFC is involved in cognitive empathy.[42] The Default Mode Network (DMN) is a network classically observed during resting state and mind wandering. The DMN is mainly composed of the ventral MFC, the posterior cingulate cortex, and the lateral parietal cortex.[43,44] The main hub of the DMN in the ventral MFC is located in the anterior part of the IRS, in other words, anterior part of BA10/12.[13] BA10/11/12 in the region of the ventral MFC is involved in moral cognition.[45,46] BA11/12 in the region of the ventral MFC is involved in facial emotion cognition.[47]

The sulcal patterns of the ventral MFC are diverse.[2–13] However, what contributes to that diversity is summarized as follows. One is the frequency of the occurrence of PCS, the second is the connection patterns between the SRS and the CS or PCS, and the third is the frequency of the occurrence of sulcus ventral to the IRS. According to the previous study, the PCS is present in 24–68% of cases and is more frequently found in the left hemisphere.[5,7,10] The anterior origin of the CS or the PCS with a connection to the SRS is present in 21–86%.[5,12] The sulcus ventral to the IRS is present in 64–70%.[12,13] Therefore, exactly which gyrus MFC2-5 corresponds to depends on such sulcal patterns. And the relationship between each gyrus on the ventral MFC and BA is as follows. BA11 is contained in the ventral region of SG (or SG1), BA12 is in the dorsal region of SG (or SG2), BA10 is mainly in the imSFG, BA32 is mainly in the PCG, and a part of BA32 may be contained in the smSFG or the imSFG. BA24 is mainly contained in the CG (Fig. 1a). Although it is difficult to accurately identify which BA MFC2-5 corresponds to during dissection of IHA, it can be estimated to some extent from our results. In cases which both MFC1 and MFC2 are large (Type A), the dorsal region of MFC1 is likely to include BA12, and MFC2 is likely to include BA10/32. In other cases, the dorsal region of MFC1 may include BA12, MFC2 is likely to include either BA12 or BA10, MFC3 is likely to include either BA10 or BA32, and MFC4-5 is likely to include BA32 and BA24. These results are useful for careful dissection while recognizing the function of the dissected gyrus in IHA from the viewpoint of preserving higher mental functions.

Although there were some variations in IHA to treat anterior communicating artery aneurysms (Aco AN),[48–50] they have been mainly classified into two approaches according to the range and direction of dissection of the ventral MFC. One is an anterior interhemispheric approach (AIHA)[51–54] and the other is a BIHA.[55,56] AIHA is the standard surgical approach for Aco AN.[51,52,54,57–60] Dissection of the IHF in this approach is performed according to the three-step procedure described by Itoh et al.[51,52] The first step is dissection of the anterior portion of the pericallosal cistern located in front of the genu of the CC and the exposure of the pericallosal artery. The second step is that the dissection of the IH fissure proceeds anteriorly, inferiorly toward the planum sphenoidale from this anterior portion of the pericallosal cistern. The third step is the dissection between the MFC1 (SG)s posteriorly to reach the tuberculum sellae and the dissection of the cistern of lamina terminalis to expose the distal portion of the Aco complex according to the location and the size of the Aco AN. Finally, the Aco complex and the AN should be carefully dissected to complete occlusion of the aneurysmal neck. In other words, in AIHA, it is necessary to dissect almost the entire ventral MFC (MFC1-CG) (Fig. 3a).

On the other hand, in BIHA described by Yasui et al,[55,56] the craniotomy is extended further into the anterior medial part of the frontal base and the nasal bones. The dissection of the IHF proceeds directly toward the planum sphenoidale and the tuberculum sellae. The direction of the dissection is changed toward the upper Aco complex without dissecting the pericallosal cistern. In other words, in original BIHA, the range of dissection is only 1 or 2 gyri of the outermost layer of the MFC (MFC1-2)[55,56,61,62] (Fig. 3b). The advantages of BIHA are that the range of dissection is smaller than an AIHA and the operation time becomes shorter. However, such a range of dissection is not sufficient for cases of high-positioned or large Aco AN. Therefore, the procedures similar to the three steps of AIHA have been adopted in BIHA.[61–65] The first step is dissection toward the anterior portion of the pericallosal cistern, similar to AIHA, but it is not always necessary to proceed the dissection to this cistern. The second and the third steps are exactly the same as an AIHA (Fig. 3c). In this method, in cases of high-positioned or large Aco AN, after all, it is often necessary to dissect almost the entire ventral MFC (MFC1-CG) like AIHA. On the other hand, in many cases of not high-positioned and not large Aco AN, it is not necessary to dissect the entire ventral MFC. However, it is unclear how much range of the MFC should be dissected, in other words, there are no established landmarks to determine the range of dissection of the MFC required to reach just around
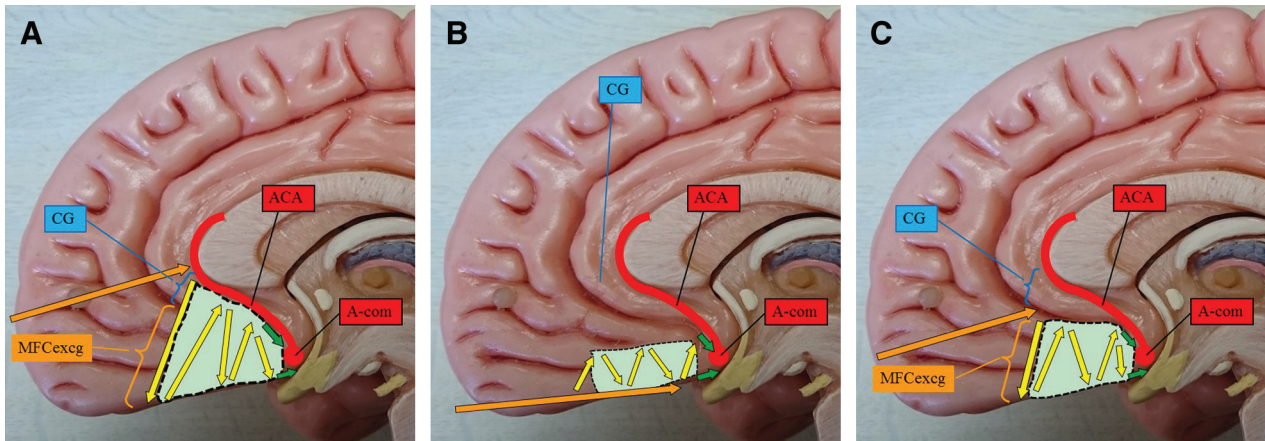
Fig. 3 Three-step procedure of the dissection in an IH approach. (A) Anterior IHA. (B, C) Variations of dissection in a basal IHA. The orange arrow shows the first step of dissection. The yellow arrows show the second steps of dissection. The green arrows show the third step of dissection. The area of light blue shows the range of dissection. ACA: anterior cerebral artery, A-com: anterior communicating artery, IHA: interhemispheric approach.

the upper portion of the cistern of lamina terminalis located distal to the Aco complex in the operative field. According to a few reports, approximately 2 gyri of the MFC or from the anterior skull base upward approximately 2 cm seems to be sufficient range of dissection in BIHA, based on their experiences.[61,63,65] However, the dissection of only 2 gyri of the outermost layer of the MFC is often difficult for inexperienced surgeons because it is necessary to dissect more carefully between the bilateral MFG with tight adhesion in the narrow operative field. And such a range of dissection is often insufficient in cases of high-positioned or large Aco AN. In our experiences, the dissection of 3 or 4 gyri of the outermost layer of the MFC has been sufficient to safely reach just around the upper portion of the cistern of lamina terminalis located distal to the Aco complex in BIHA (Fig. 4).

From the morphology of the ventral MFC, theoretically the dissection of the entire MFC excluding CG is sufficient to safely reach the upper portion of the cistern of lamina terminalis located distal to the Aco complex in BIHA (Fig. 3c). Therefore, intraoperative identification of the range of MFCexcg provides the surgeons good intraoperative orientation not only in BIHA but also in AIHA. And knowledge of the sulcal patterns of MFC is important to determine the range of MFCexcg. The pattern of bilateral MFCexcg consisting of 3 gyri or more was observed in approximately 85% of the cadavers, that is, the CG corresponds to the fourth or fifth gyrus from the outermost layer in the subcallosal portion. Thus, the dissection of at least the outermost 3 or 4 gyri of both MFC is likely to be sufficient to safely reach the upper portion of the cistern

of lamina terminalis located distal to the Aco complex in BIHA (Fig. 4). However, the pattern of either MFCexcg consisting of 2 gyri was observed in about 15% of cadaveric cases. The mean width of the MFC1 (8.3±.3d mm) and that of the MFC2 (6.8±.8d mm) were larger in this pattern. In the cases that both MFC1 and MFC2 are developed and large, the CG corresponds to the third gyrus from the outermost layer in the subcallosal portion with a high probability. Thus, in these cases, dissection of the outermost 2 gyri of the MFC is likely to be sufficient to safely reach just around the upper portion of the cistern of lamina terminalis in BIHA as well. The mean width of the MFCexcg in the subcallosal portion in all specimens was 20.6±3.4 mm, although this measured value was based on cadaver specimens and is somewhat smaller than that in actual living brains. As a result, we conclude that the dissection from the base of the SG upward to about 2 cm, the dissection of the outermost 3 or 4 gyri of the MFC in many cases, and the dissection of the outermost 2 gyri of the MFC in cases of both large MFC1 and MFC2 become landmarks to safely reach the upper portion of the cistern of lamina terminalis located distal to the Aco complex in BIHA. These results are quite consistent with our experiences and previous reports. Although the actual range of MFC dissection in BIHA depends on the adhesion of IHF, and the height, size, and location of the Aco AN, understanding of the anatomical relationship between the MFC and the Aco complex are useful to obtain intraoperative good orientation, and to increase the safety and efficiency of dissection not only in BIHA but also in AIHA.
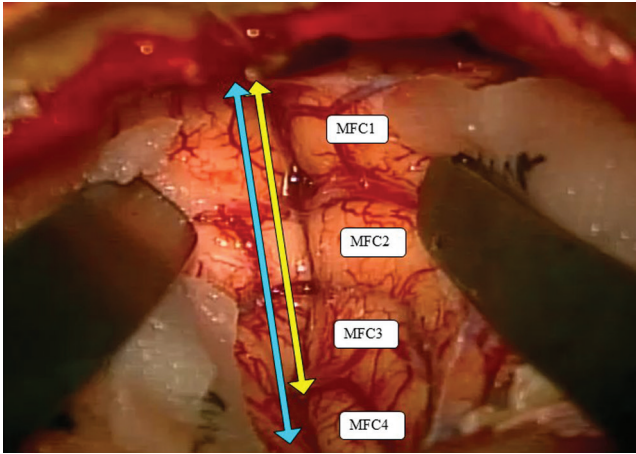
Fig. 4 The actual operative view of the MFCexcg in IHA. The yellow two-way arrow shows the outermost 3 gyri of the MFC in the subcallosal portion. The light blue two-way arrow shows the outermost 4 gyri of the MFC in the subcallosal portion. MFC: medial frontal cortex.

Conclusions

It is useful to understand the morphological features of the MFC to obtain intraoperative good orientation in an IHA.

Conflicts of Interest Disclosure

The authors report no conflict of interest concerning the materials or methods used in this study or the findings specified in this paper.

References

1) Hiser J, Koenigs M: The multifaceted role of the ventromedial prefrontal cortex in emotion, decision making, social cognition, and psychopathology. *Biol Psychiatry* 83: 638–647, 2018

2) Fornito A, Yücel M, Wood S, et al.: Individual differences in anterior cingulate/paracingulate morphology are related to executive functions in healthy males. *Cereb Cortex* 14: 424–431, 2004

3) Fornito A, Whittle S, Wood SJ, Velakoulis D, Pantelis C, Yücel M: The influence of sulcal variability on morphometry of the human anterior cingulate and paracingulate cortex. *Neuroimage* 33: 843–854, 2006

4) Fornito A, Wood SJ, Whittle S, et al.: Variability of the paracingulate sulcus and morphometry of the medial frontal cortex: associations with cortical thickness, surface area, volume, and sulcal depth. *Hum Brain Mapp* 29: 222–236, 2008

5) Ono M, Kubik S, Abernathey C: Atlas of the Cerebral Sulci. Stuttgart: Georg Thieme Verlage, 1990, pp. 112–123

6) Paus T, Otaky N, Caramanos Z, et al.: In vivo morphometry of the intrasulcal gray matter in the human cingulate, paracingulate, and superior-rostral sulci: hemispheric asymmetries, gender differences and probability maps. *J Comp Neurol* 376: 664–673, 1996

7) Paus T, Tomaiuolo F, Otaky N, et al.: Human cingulate and paracingulate sulci: pattern, variability, asymmetry, and probabilistic map. *Cereb Cortex* 6: 207–214, 1996

8) Paus T: Primate anterior cingulate cortex: where motor control, drive and cognition interface. *Nat Rev Neurosci* 2: 417–424, 2001

9) Vogt BA, Nimchinsky EA, Vogt LJ, Hof PR: Human cingulate cortex: surface features, flat maps, and cytoarchitecture. *J Comp Neurol* 359: 490–506, 1995

10) Yücel M, Stuart GW, Maruff P, et al.: Hemispheric and gender-related differences in the gross morphology of the anterior cingulate/paracingulate cortex in normal volunteers: an MRI morphometric study. *Cereb Cortex* 11: 17–25, 2001

11) Mackey S, Petrides M: Quantitative demonstration of comparable architectonic areas within the ventromedial and lateral orbital frontal cortex in the human and the macaque monkey brains. *Eur J Neurosci* 32: 1940–1950, 2010

12) Mackey S, Petrides M: Architecture and morphology of the human ventromedial prefrontal cortex. *Eur J Neurosci* 40: 2777–2796, 2014

13) Lopez-Persem A, Verhagen L, Amiez C, Petrides M, Sallet J: The human ventromedial prefrontal cortex: sulcal morphology and its influence on functional organization. *J Neurosci* 39: 3627–3639, 2019

14) Ardeshiri A, Ardeshiri A, Wenger E, Holtmannspötter M, Winkler PA: Surgery of the anterior part of the frontal lobe and of the central region: normative morphometric data based on magnetic resonance imaging. *Neurosurg Rev* 29: 313–320; discussion 320–321, 2006

15) Imada Y, Yuki K, Migita K, Sadatomo T, Kuwabara M: Prediction of the intraoperative location of the anterior communicating artery using medical frontal gyrus as a landmark in an interhemispheric approach. *Jpn Neurosurg* 22: 459–466, 2013

16) Brodmann K: Vergleichende Lokalisationslehre der Grosshirnrinde in ihren prinzipien dargestellt auf Grund des Zellenbaues. Leipzig: Barth, 1909

17) Brodmann K. Fienere Anatomie des Grosshirns. In: Lewandowsky M, et al, editors. *Handbuch der Neurologie*. Berlin: Springer J, 1910, pp. 206–307

18) Economo C: The cytoarchitectonics of the human cerebral cortex. London: Oxford University Press, 1929

19) ten Donkelaar HJ, Tzourio-Mazoyer N, Mai JK: Toward a common terminology for the gyri and sulci of the human cerebral cortex. *Front Neuroanat* 12: 93, 2018

20) Devinsky O, Morrell MJ, Vogt BA: Contributions of anterior cingulate cortex to behaviour. *Brain* 118: 279–306, 1995

21) Hänsel A, von Känel R: The ventro-medial prefrontal cortex: a major link between the autonomic nervous

system, regulation of emotion, and stress reactivity? *Biopsychosoc Med* 2: 21, 2008

22) Vogt BA, Finch DM, Olson CR: Functional heterogeneity in cingulate cortex: the anterior executive and posterior evaluative regions. *Cereb Cortex* 2: 435–443, 1992

23) Gallagher HL, Happé F, Brunswick N, Fletcher PC, Frith U, Frith CD: Reading the mind in cartoons and stories: an fMRI study of 'theory of mind' in verbal and nonverbal tasks. *Neuropsychologia* 38: 11–21, 2000

24) Atlas LY, Wager TD: A meta-analysis of brain mechanisms of placebo analgesia: consistent findings and unanswered questions. *Handb Exp Pharmacol* 225: 37–69, 2014

25) Eippert F, Bingel U, Schoell ED, et al.: Activation of the opioidergic descending pain control system underlies placebo analgesia. *Neuron* 63: 533–543, 2009

26) Bingel U, Lorenz J, Schoell E, Weiller C, Büchel C: Mechanisms of placebo analgesia: rACC recruitment of a subcortical antinociceptive network. *Pain* 120: 8–15, 2006

27) Ramnani N, Owen AM: Anterior prefrontal cortex: insights into function from anatomy and neuroimaging. *Nat Rev Neurosci* 5: 184–194, 2004

28) Burgess PW, Veitch E, de Lacy Costello A, Shallice T: The cognitive and neuroanatomical correlates of multitasking. *Neuropsychologia* 38: 848–863, 2000

29) Koechlin E, Corrado G, Pietrini P, Grafman J: Dissociating the role of the medial and lateral anterior prefrontal cortex in human planning. *Proc Natl Acad Sci U S A* 97: 7651–7656, 2000

30) Burgess PW, Gilbert SJ, Dumontheil I: Function and localization within rostral prefrontal cortex (area 10). *Philos Trans R Soc Lond B Biol Sci* 362: 887–899, 2007

31) Okuda J, Fujii T, Ohtake H, et al.: Differential involvement of regions of rostral prefrontal cortex (Brodmann area 10) in time- and event-based prospective memory. *Int J Psychophysiol* 64: 233–246, 2007

32) Reynolds JR, McDermott KB, Braver TS: A direct comparison of anterior prefrontal cortex involvement in episodic retrieval and integration. *Cereb Cortex* 16: 519–528, 2006

33) Knutson B, Fong GW, Bennett SM, Adams CM, Hommer D: A region of mesial prefrontal cortex tracks monetarily rewarding outcomes: characterization with rapid event-related fMRI. *Neuroimage* 18: 263–272, 2003

34) Koenigs M, Tranel D: Irrational economic decision-making after ventromedial prefrontal damage: evidence from the Ultimatum Game. *J Neurosci* 27: 951–956, 2007

35) Koenigs M, Young L, Adolphs R, et al.: Damage to the prefrontal cortex increases utilitarian moral judgements. *Nature* 446: 908–911, 2007

36) Lebreton M, Jorge S, Michel V, Thirion B, Pessiglione M: An automatic valuation system in the human brain: evidence from functional neuroimaging. *Neuron* 64: 431–439, 2009

37) Camille N, Griffiths CA, Vo K, Fellows LK, Kable JW: Ventromedial frontal lobe damage disrupts value maximization in humans. *J Neurosci* 31: 7527–7532, 2011

38) Grabenhorst F, Rolls ET: Value, pleasure and choice in the ventral prefrontal cortex. *Trends Cogn Sci* 15: 56–67, 2011

39) Liu X, Hairston J, Schrier M, Fan J: Common and distinct networks underlying reward valence and processing stages: a meta-analysis of functional neuroimaging studies. *Neurosci Biobehav Rev* 35: 1219–1236, 2011

40) Levy DJ, Glimcher PW: The root of all value: a neural common currency for choice. *Curr Opin Neurobiol* 22: 1027–1038, 2012

41) Pujara MS, Philippi CL, Motzkin JC, Baskaya MK, Koenigs M: Ventromedial prefrontal cortex damage is associated with decreased ventral striatum volume and response to reward. *J Neurosci* 36: 5047–5054, 2016

42) Shamay-Tsoory SG, Aharon-Peretz J, Perry D: Two systems for empathy: a double dissociation between emotional and cognitive empathy in inferior frontal gyrus versus ventromedial prefrontal lesions. *Brain* 132: 617–627, 2009

43) Davey CG, Pujol J, Harrison BJ: Mapping the self in the brain's default mode network. *Neuroimage* 132: 390–397, 2016

44) Raichle ME: The brain's default mode network. *Annu Rev Neurosci* 38: 433–447, 2015

45) Young L, Koenigs M: Investigating emotion in moral cognition: a review of evidence from functional neuroimaging and neuropsychology. *Br Med Bull* 84: 69–79, 2007

46) Fumagalli M, Priori A: Functional and clinical neuroanatomy of morality. *Brain* 135: 2006–2021, 2012

47) Tsuchida A, Fellows LK: Are you upset? Distinct roles for orbitofrontal and lateral prefrontal cortex in detecting and distinguishing facial expressions of emotion. *Cereb Cortex* 22: 2904–2912, 2012

48) Fukushima T, Miyazaki S, Takusagawa Y, Reichman M: Unilateral interhemispheric keyhole approach for anterior cerebral artery aneurysms. *Acta Neurochir Suppl (Wien)* 53: 42–47, 1991

49) Kikuchi K, Watanabe K: Modified bifrontal interhemispheric approach to aneurysms of the anterior communicating artery with the use of a trephine craniotomy. A review of personal experience with 25 cases. *Acta Neurochir (Wien)* 125: 127–131, 1993

50) Yeh H, Tew JM: Anterior interhemispheric approach to aneurysms of the anterior communicating artery. *Surg Neurol* 23: 98–100, 1985

51) Ito Z: The microsurgical anterior interhemispheric approach suitably applied to ruptured aneurysms of the anterior communicating artery in the acute stage. *Acta Neurochir (Wien)* 63: 85–99, 1982

52) Ito Z: Microneurosurgery of Cerebral Aneurysms. Atlas by Zentaro Ito. Niigata: Nishimura-Elsevier, 1985

53) Lougheed WM: Selection, timing, and technique of aneurysm surgery of the anterior circle of Willis. *Clin Neurosurg* 16: 95–113, 1969

54) Suzuki J, Mizoi K, Yoshimoto T: Bifrontal interhemispheric approach to aneurysms of the anterior communicating artery. *J Neurosurg* 64: 183–190, 1986

55) Yasui N, Suzuki A, Sayama I, Kawamura S: A basal interhemispheric operative approach for anterior communicating artery aneurysms. *Neurol Med Chir (Tokyo)* 27: 756–761, 1987

56) Yasui N, Nathal E, Fujiwara H, Suzuki A: The basal interhemispheric approach for acute anterior communicating aneurysms. *Acta Neurochir (Wien)* 118: 91–97, 1992

57) Kamiyama H: Topographical microanatomy for anterior interhemispheric approach – Microstructure of arachnoid membrane and trabeculae: Surgical Anatomy for Microneurosurgery III – Cistern, Fissure and Sulcus-. Tokyo: SciMed Publications, 1991, pp. 39–49

58) Nishi T: Interhemispheric approach for anterior communicating aneurysm. *Curr Pract Neurosurg Practical Currently* 17: 546–557, 2007 (Japanese)

59) Noda K, Tanikawa R, Kamiyama H, Ohta N, Yabuuchi T, Miyata S: Interhemispheric approach for ACom aneurysm. *Jpn J Neurosurg* 21: 834–841, 2012 (Japanese)

60) Tanikawa R: Less invasive cisternal approach and removal of subarachnoid hematoma for the treatment of ruptured cerebral aneurysms. *No Shinkei Geka* 35: 17–24, 2007 (Japanese)

61) Ishikawa T: Clipping of anterior communicating aneurysm. *Curr Pract Neurosurg Practical Currently* 20: 890–900, 2010 (Japanese)

62) Kazumata K: About interhemispheric approach. *Curr Pract Neurosurg Practical Currently* 21: 1202–1206, 2011 (Japanese)

63) Moroi J: Clipping of anterior communicating aneurysm in the basal interhemispheric approach. *Curr Pract Neurosurg Practical Currently* 22: 14–22, 2012 (Japanese)

64) Sakata Y, Hadeishi H: Basal interhemispheric approach for anterior communicating aneurysms. *Jpn J Neurosurg* 19: 720–726, 2010 (Japanese)

65) Suzuki A, Yasui N: Interhemispheric approach to the anterior communicating artery aneurysm. *Jpn J Neurosurg* 1: 218–225, 1992 (Japanese)

Corresponding author: Yasutaka Imada, MD, PhD
Department of Neurosurgery, Yamada Memorial Hospital, 6-2-1 Miyaura, Mihara, Hiroshima 723-0051, Japan.
e-mail: yasutaka5682@yahoo.co.jp